Visible Light Communication Using OFDM

Mostafa Z. Afgani, Harald Haas, Hany Elgala, and Dietmar Knipp
School of Engineering and Science
International University Bremen
28759 Bremen, Germany
Email: {m.afgani,h.haas,h.elgala,d.knipp}@iu-bremen.de

Abstract— **In this paper wireless communication using white, high brightness LEDs (light emitting diodes) is considered. In particular, the use of OFDM (orthogonal frequency division multiplexing) for intensity modulation is investigated. The high peak-to-average ratio (PAR) in OFDM is usually considered a disadvantage in radio frequency transmission systems due to non-linearities of the power amplifier. It is demonstrated theoretically and by means of an experimental system that the high PAR in OFDM can be exploited constructively in visible light communication to intensity modulate LEDs. It is shown that the theoretical and the experimental results match very closely, and that it is possible to cover a distance of up to one meter using a single LED.**

I. Introduction

Recently, there has been increased interest in visible light communication systems. The research is motivated by an increasing need of indoor communication systems and the improvements of light emitting diode technologies (LEDs). High brightness LEDs are already used for several applications and it is foreseen that they will also replace conventional lighting sources in the next decade. Furthermore, the bandwidth of optical free space communication systems using LED technology is high in comparison to radio frequency based solutions. This widespread use provides the necessary infrastructure and hence removes one of the major hurdles faced by new communication schemes; thus making the technology particularly appealing. A typical application scenario might be to additionally use the reading lights in planes for high speed wireless transmission. Moreover, some of the notable advantages of visible light communication over RF (radio frequency) and IR (infra red) based systems are:

- There are no regulations regarding the use of the visible EM (electromagnetic) spectrum
- Unlike IR communication schemes, there are no health regulations to restrict the transmit power
- Optical communication provides higher security than RF communication schemes; it is very difficult for an intruder to (covertly) pick up the signal from outside the room

In an optical communication system, it is possible to modulate the transmitted optical signal in a variety of ways. The phase/frequency, polarization, or the intensity of the optical signal can be modulated. Intensity modulation has the advantage of being particularly easy to implement; the optical output power of the source is simply varied according to the modulating signal. The optical signal thus produced is also easy to detect - the modulating signal is easily recovered from the output of a photodiode. The method is therefore aptly termed *direct-detection*. The penalty for the simplicity of IM-DD (intensity modulation - direct detection) systems is a reduction in sensitivity, and the vulnerability to noise – as compared to coherent detection methods (e.g. heterodyning).

OOK (on-off keying), PCM (pulse code modulation), and SC-BPSK (sub-carrier binary phase shift keying) are some of the more popular modulation schemes used in conjunction with LED wireless systems [1]. The use of OFDM was first noted in [2]. The inherent robustness of OFDM against multipath effects makes it an excellent choice for situations where multiple transmitters are used simultaneously (to avoid shadowing effects) and a path difference to the receiver exists. One of the major disadvantages of an OFDM based system is the characteristic high crest factor of the time domain signal. In traditional RF based systems, this usually necessitates a transmitter with a high dynamic range and hence results in reduced power efficiency. In the proposed optical LED system, this disadvantage is turned to an advantage - the time domain OFDM signal is used to modulate (IM-DD) the optical source. The signal variations are around an operating point determined by the particular LED in use. It is chosen such that the LED operates in the linear region of the current vs. intensity curve.

Most of the research in the area of visible light communication using OFDM has been theoretical. The goal of the project is to implement an experimental system. This experimental system is primarily aimed at demonstrating a proof-of-concept for the approach of exploiting the high crest-factor in OFDM for LED intensity modulation. Therefore, standard off-the-shelf components were selected. Thereby, it is accepted that the system is clearly not optimised for maximum data rate transmission capabilities. Such optimisation will be carried out at later stages once the feasibly has be shown.

In the next section, the system design and the optical setup is described. The theoretical and experimental results are described in Section III. Section IV concludes the paper.

II. System Design

The communication chain is implemented using a pair of digital signal processing development kits (Texas Instruments TMS320C6711). The D/A converters of the boards have a precision of 16 bits and operate at a frequency of 8kHz – offering a maximum system bandwidth of 4kHz and a sampling interval of 125μs. The on-board DSP is capable of floating point operations. With a 64-point IFFT (inverse

1-4244-0106-2/06/$20.00 ©2006 IEEE

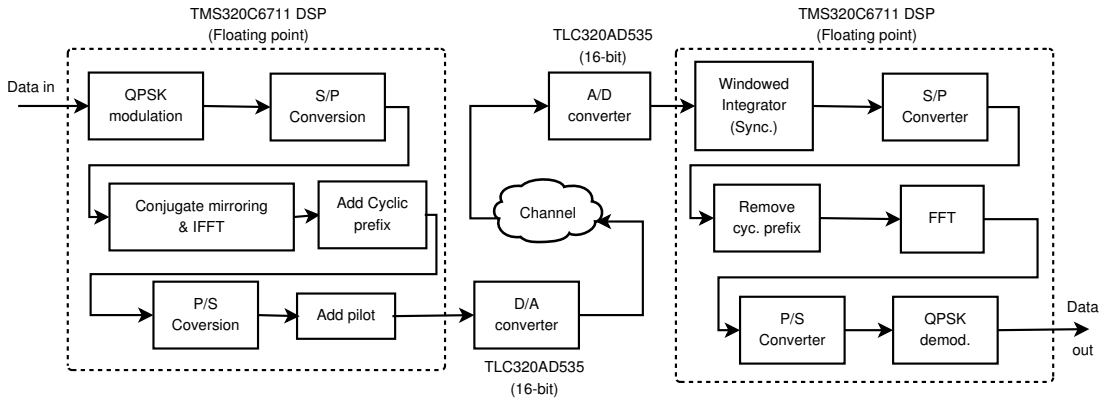

Fig. 1. Block diagram of the OFDM communication chain

0	a	b	c	d	$\cdots$	0	$\cdots$	d*	c*	b*	a*

Fig. 2. Sample IFFT input frame (transposed)

fast Fourier transform) the duration of an OFDM symbol is $(64 \times 125\mu s =)$ $0.008s$. With QPSK (quadrature phase shift keying) modulation, the maximum number of bits transferable by each OFDM symbol is then $(64 \times 2 =)$ 128. The ideal system is then capable of a maximum raw (assuming no guard or pilot, and all subcarriers are modulated by independent data streams) data rate of $\left(\frac{128}{0.008} =\right)$ 16kbps. However, with the IFFT framing structure chosen for the implementation, the maximum achievable data rate (assuming no guard or pilot) is approximately 8kbps.

The following is a description of the various blocks of the chain. Fig. 1 shows a block diagram of the scheme implemented.

A. Transmitter

The transmitter consists of a file processor, QPSK modulator, and an OFDM modulator. The file processor accepts an ASCII data file consisting of the binary data stream. The data read from the file is encoded using the QPSK modulation scheme by means of a lookup table:

$$\begin{array}{ll} 00 \Rightarrow & \texttt{1 + j} \\ 01 \Rightarrow & \texttt{1 - j} \end{array} \qquad \begin{array}{ll} 10 \Rightarrow & \texttt{-1 + j} \\ 11 \Rightarrow & \texttt{-1 - j} \end{array}$$

The symbols then undergo a serial to parallel conversion in preparation for the IFFT operation. The parallel data stream is then used to design the data frame for the IFFT. The first element of the data frame represents the DC value and hence is chosen to be zero. If the number of subcarriers is M, and the IFFT size is N, then elements 2 to $M+1$ of the frame consist of the parallel data and elements $N-M+1$ to N consist of the conjugate complex and mirrored version of the data. If $N > 2M+1$, the intermediate elements are zero. $N < 2M+1$ is not feasible and hence the condition $N \geq 2M+1$ must be strictly enforced. When $N = 2M+1$, there are no intermediate zero elements. The transpose of a sample frame is shown in Fig. 2. For the simple one LED transmitter, this is necessary to ensure that the output from the IFFT operation is real valued. In favour of simplicity, the resulting reduction in the spectral efficiency by a factor of two is accepted – again, this setup should primarily provide a proof-of-concept. Many white LEDs are in effect a combination of red, green and blue LEDs and hence, it is also possible to use the regular data frame structure (no complex conjugate mirroring) and modulate two of the three LEDs to transmit the real and imaginary parts of the resulting complex OFDM symbols separately. The third LED can be left active but unmodulated to maintain "whiteness". Of course the two LEDs can also be used with the modified IFFT frame structure to provide full-duplex communication. The receiver would then also have to employ two photo-diodes – each filtered to be sensitive to the wavelength of one of the LEDs. Once the IFFT operation is carried out, the output is processed to append a 5μs cyclic prefix for protection against multipath effects. The guard length was chosen such that any such effects can be safely ignored. Once the prefix has been added, the parallel data stream is converted back into a serial stream. Before the OFDM symbols are transmitted via the D/A converter, a pilot sequence is transmitted. The sequence is one OFDM symbol long and consists of two complete sinusoids separated by zeros (Fig. 4). The peak-to-peak amplitude of these "guard sinusoids" is approximately 2.5V and hence they are as strong as the strongest data signal in the time domain waveform. This special structure is needed for successful synchronization at the receiver. The synchronization procedure is detailed in Section II-B. The transmitter then stops processing further data and repeatedly transmits the sequence of OFDM symbols and the pilot until a feedback from the receiver is obtained via a wired return channel. Once the transmitter reaches the end of the ASCII data file, it transmits a predefined bit pattern to signal the end of file to the receiver and stops. An OFDM time domain signal depicting the typically high peak-to-average ratio is shown in Fig. 3.

B. Receiver

The receiver starts by capturing a data stream two frames long. This ensures that the captured data contains at least one

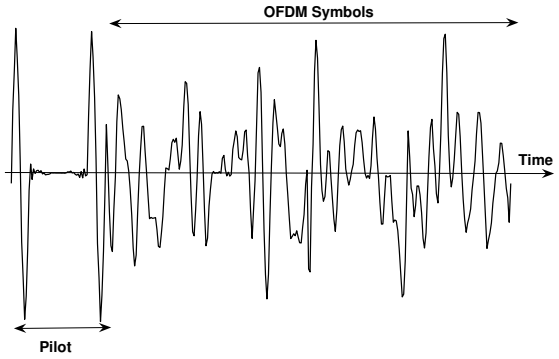

Fig. 3. A Typical Time Domain Signal

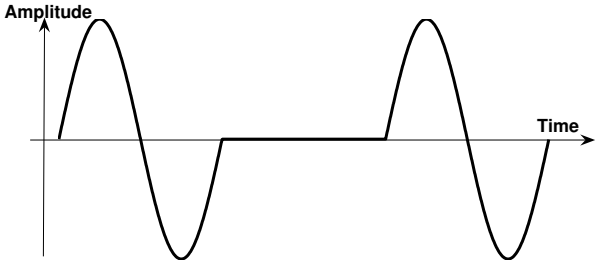

Fig. 4. The Pilot Symbol

contiguous frame (one pilot symbol and OFDM symbols). Once the symbols have been captured, the receiver signals the transmitter to continue processing the next set of data. The captured symbols are then run through a synchronization detection subroutine. The detector is essentially a running integrator with a window size equal to the length of the silent period (zeros) in the pilot symbol. The integrator scans through the absolute value of the captured data stream one sample at a time and records the index of the position where the minimum value of the integral was observed. As the integrator only considers absolute values, the integral over a sinusoid is a non-zero number. At this point the advantage of the special pilot structure becomes clear – the guard sinusoids provide an effective contrast between themselves and the silent period and hence make it easier for the detector to reach the correct decision. Eventually, the integrator window will come into alignment with the silent portion of a pilot symbol and it is here that the lowest integral will be recorded. Thus the index to the start of the OFDM symbols is determined. Then, using this index, the OFDM symbols are extracted and run through the serial to parallel converter. Once the data is parallelized, the cyclic prefix is removed and the frame is passed to the FFT operator. The FFT operation reproduces the mirrored frame structure designed in the transmitter. The upper half (elements 2 to $M+1$) of this frame is retained as the valid result. The complex data is then passed through the QPSK demodulator to recover the binary data. The decision regions defined are:

$$\begin{aligned}
\mathbb{R}(symbol) > 0 \quad \& \quad \mathbb{C}(symbol) > 0 \Rightarrow 00 \\
\mathbb{R}(symbol) < 0 \quad \& \quad \mathbb{C}(symbol) > 0 \Rightarrow 10 \\
\mathbb{R}(symbol) > 0 \quad \& \quad \mathbb{C}(symbol) < 0 \Rightarrow 01 \\
\mathbb{R}(symbol) < 0 \quad \& \quad \mathbb{C}(symbol) < 0 \Rightarrow 11
\end{aligned}$$

The QPSK symbols are also written to an ASCII file to facilitate the plotting of receiver constellation diagrams. Once the binary data has been recovered, it is written to an ASCII data file. Since the transmitted bits are known to the receiver, a bit error rate (BER) calculation is also carried out. At every cycle the receiver checks the received bit sequences for a match against the *end of file* bit pattern; if a match is found, the files are closed and the receiver stops. Otherwise, the program captures the next set of data and repeats the signal processing.

It is assumed that the channel is single tap with a real coefficient and hence is flat fading. Therefore any phase/amplitude distortion is assumed to be minimal. Consequently, an equalizer would have very little effect on the final result and hence was omitted from the design of this simple transmission chain.

C. The Optical Channel

For the theoretical analysis a suitable channel model is required. The channel model used is that proposed by Barry et al. [3]. For the line of sight (LOS) case with no reflections and assuming that the source and receiver separation squared (R^2) is much greater than the receiver area (A_R), the channel impulse response can be approximated by a scaled and delayed Dirac delta function

$$h\left(t;\mathcal{S},\mathcal{R}\right) \approx \frac{n+1}{2\pi}\cos^{n}\left(\phi\right) d\Omega \,\mathrm{rect}\left(\frac{\theta}{\mathrm{FOV}}\right)\delta\left(t-\frac{R}{c}\right) \tag{1}$$

where $\mathcal{S}$ is the source and $\mathcal{R}$ is the receiver. The simple source is defined as $\mathcal{S} = \{\mathbf{r}_S, \hat{\mathbf{n}}_S, n\}$; $\mathbf{r}_S$ is the position, $\hat{\mathbf{n}}_S$ is the orientation, and n is the mode number associated with the directivity of the source and can be calculated from the source half-angle, α_H, using (2) [4]. The simple detector is defined as $\mathcal{R} = \{\mathbf{r}_R, \hat{\mathbf{n}}_R, A_R, FOV\}$; $\mathbf{r}_R$ is the position, $\hat{\mathbf{n}}_R$ is the orientation, A_R the receiver area, and FOV the field of vision.

$$\alpha_H = \cos^{-1}\left(0.5\right)^{\frac{1}{n}} \tag{2}$$

$d\Omega$ is defined as the solid angle subtended by the receiver's differential area

$$d\Omega \approx \cos\left(\theta\right)\frac{A_R}{R^2} \tag{3}$$

θ is the angle between $\hat{\mathbf{n}}_R$ and $(\mathbf{r}_S - \mathbf{r}_R)$

$$\cos\left(\theta\right) = \hat{\mathbf{n}}_R \cdot \frac{\left(\mathbf{r}_S - \mathbf{r}_R\right)}{R} \tag{4}$$

ϕ is the angle between $\hat{\mathbf{n}}_S$ and $(\mathbf{r}_R - \mathbf{r}_S)$

$$\cos\left(\phi\right) = \hat{\mathbf{n}}_S \cdot \frac{\left(\mathbf{r}_R - \mathbf{r}_S\right)}{R} \tag{5}$$

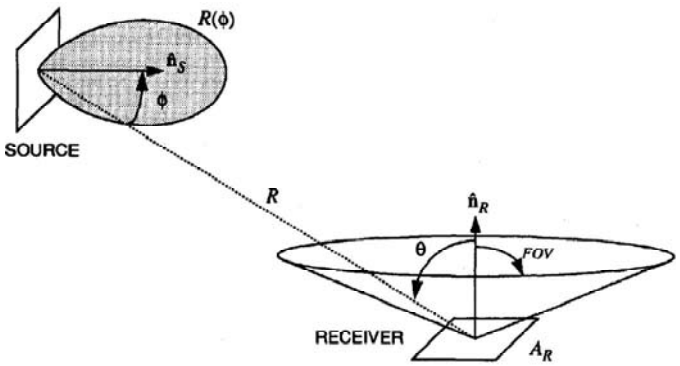

Fig. 5. Source and Detector Geometry [3]

The function $\mathrm{rect}\,(x)$ is defined as:

$$\mathrm{rect}\,(x) = \begin{cases} 1 & \text{for} \quad |x| \leq 1 \\ 0 & \text{for} \quad |x| > 1 \end{cases} \tag{6}$$

c is the speed of light. The approximation to the impulse response approaches equality as the ratio $\frac{A_R}{R^2}$ approaches zero. The source and detector geometry is best explained by Fig. 5.

Although an algorithm to derive the channel impulse response for multiple reflections is provided in [3], the influence of multiple reflections was neglected; as the $5\mu s$ guard in the OFDM symbols is more than enough to mitigate any multipath effects encountered.

At this point, it is necessary to note that the channel equation

$$y = r \cdot (x * h) + \tilde{n} \tag{7}$$

relates the transmitted *power* to the received *current*. The input signal x is a power signal, the channel transfer function h is dimensionless, and the receiver responsivity factor r represents the conversion ratio between received optical power and photodiode current at the receiver. Consequently, the received signal y and the additive white Gaussian noise $\tilde{n}$ are currents. In optical channels the quality of the transmission is dominated by shot noise; the ambient light striking the detector leads to a steady shot noise that can be considered as a Gaussian noise process. The receiver pre-amplifier noise is also signal independent and Gaussian [5].

D. The Optical Interface

The optical source is a 5mm White LED with a luminous intensity of 5600 mcd. At the normal operational point of the LED, the electrical power output is about 72 mW. With a 33% efficiency, the optical power output is calculated to be approximately 24 mW.

The optical detector employs a 9.8 mm^2 planar photodiode with a built in infra-red rejection filter. The FOV is 60° and the directional sensitivity at 0° is unity. The optical receiver output is biased by +1.5V to ensure that the signal input to the receiver DSP codec falls within the prescribed -0.3V to +3.6V range. Fig. 6 shows a typical setup.

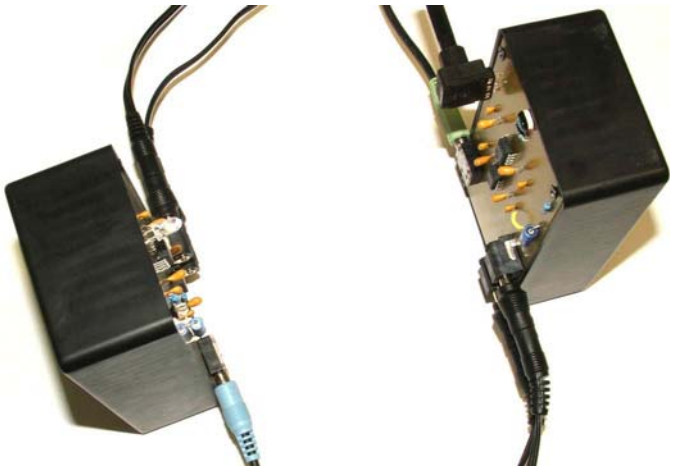

Fig. 6. The Optical Interface

III. Theoretical & Experimental Results

In order to compare the experimental findings with theoretical results, a MATLAB simulation chain was designed. In order to simplify the experiments only direct LOS conditions were considered; i.e. $\theta = 0^\circ$ and $\phi = 0^\circ$. For the simulation chain, time delay in the single path LOS channel is irrelevant since there are no multipath delayed components to consider; therefore, the $\delta\left(t - \frac{R}{c}\right)$ term drops from (1) and leaves an impulse response that is a scalar. As a result, the effect of the channel is fully represented by the channel DC gain

$$H\,(0) = \int_{-\infty}^{\infty} h\,(t)\ dt \tag{8}$$

For the intensity-in intensity-out channel, this is the fraction of the power from a continuous wave transmitter that reaches the detector [3].

A number of physical parameters such as the source mode number, n, and the responsivity of the photodiode to white light, r, were not available from the datasheets and hence had to be experimentally determined and/or calculated. The datasheet for the white LED specifies a beam half-angle (α_H) of 20°. Hence, using (2) the mode number is calculated as 45. In order to determine the responsivity of the photodiode to white light from the LED, the current generated in response to varying receiver-transmitter separations were noted. Since the total optical power transmitted from the optical point source is known, it is possible to calculate the power density (W/m^2) over a surface at any arbitrary distance. The first step is to determine the beam solid angle φ (steradians) given the beam half-angle α_H (radians):

$$\varphi = \pi \cdot (\alpha_H)^2 \tag{9}$$

Then the surface area subtended by φ at a distance R is φR^2. The source is left unmodulated and hence has a constant optical power output P_T. The power density at an arbitrary distance R is then $\frac{P_T}{\varphi R^2}$. Denoting the received current as I_R, the expression for the current density at the receiver in

TABLE I

MEASURED P_N [dBW] values for different scenarios

Scenario	$\mathbf{P_N}$ [dBW]
Dark Room	-71.6372
Fluorescent Lighting	-41.0672
Indoor (Diffused Sunlight)	-70.7372

response to the source is $\frac{I_R}{A_R}$. The responsivity can then be calculated as

$$r = \frac{I_R}{A_R} \times \frac{\varphi R^2}{P_T}. \tag{10}$$

Although the equation displays an apparent dependency of r on R, this, however, is not the case – the current, I_R, is proportional to $\frac{1}{R^2}$ and hence counters the effect of the R^2 term in the numerator; therefore r is a simple scalar coefficient. From the experimental data, the responsivity of the receiver to white light from the LED was calculated to be 0.03 A/W.

To study the performance of the system three typical scenarios were considered. The first experiments were carried out in a dark room. The second set were in a typical office room illuminated by fluorescent lights. The final set of results were obtained in a room illuminated by the diffused sunlight through the windows. In order to have a valid comparison between the simulated results and the experimental results, it was necessary to calculate the approximate noise levels (P_N) associated with the three scenarios. This was done by recording the signal at the absence of the transmitter. As it is assumed that this captured waveform represents a sample function of an ergodic and zero mean noise process at the receiver, the (linear) noise power in Watts was calculated as

$$P_N \approx \frac{1}{N} \cdot \sum_{i=0}^{N} y_i^2(t) \tag{11}$$

where N is the number of samples and y_i is the received waveform at sample index i. Using these values, the P_N in dBW were calculated as shown in Table I. The noise levels for the indoor and darkness scenarios are almost identical since noise in the digital circuitry is the major contributor rather than ambient optical power.

Fig. 7 shows the distance versus BER plot for the simulated and experimental results. Referring to the P_N values associated with the three scenarios (Table I), it is observed that the various curves are in agreement. The poor performance of the system under fluorescent lighting can be ascribed to the large amount of impulsive noise that is generated due to the switching nature of the fluorescent technology. As expected, the experimental performance curves are worse than the theoretical curves at the same P_N. This is to be expected since the simulation does not account for transmitter noise, loss of synchronization at higher distances, and other implementation losses.

Fig. 8 shows the signal constellations for the system in the dark and under fluorescent lighting respectively. At a distance

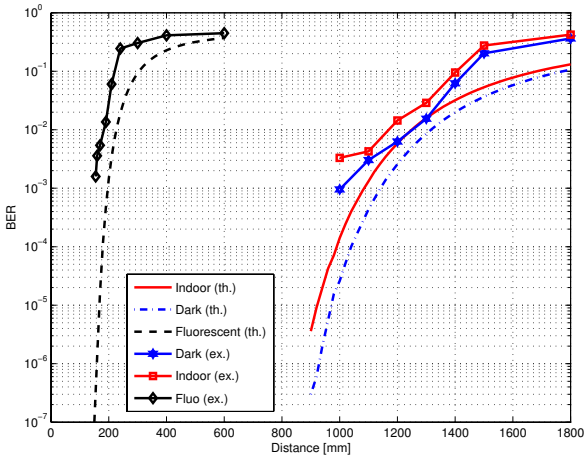

Fig. 7. Bit error rate as a function of the distance between the transmitter and the receiver

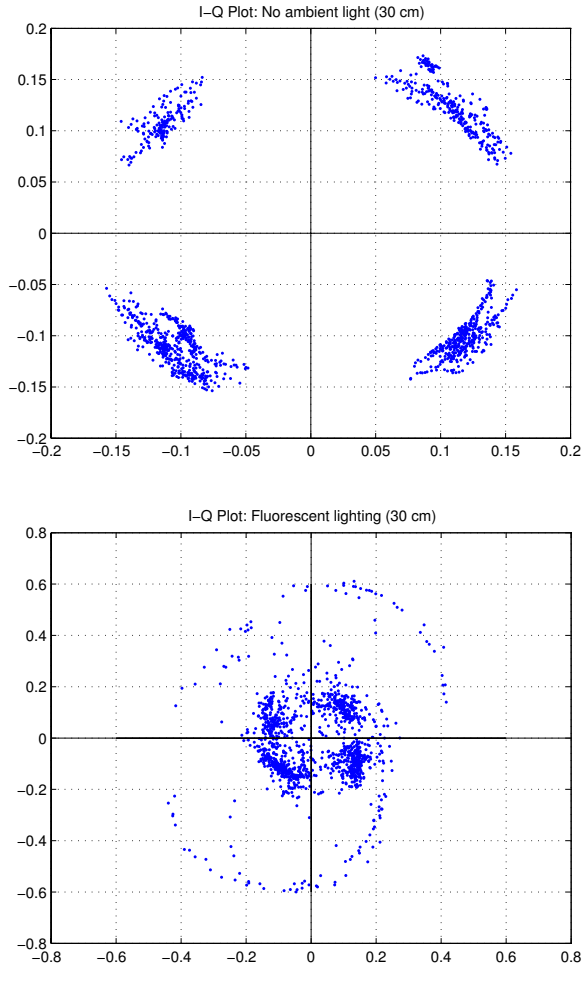

Fig. 8. Signal Constellation for QPSK Symbols Received at R = 300 mm

of 300 mm, the four regions remain quite distinct for the system in the dark. The illuminated system, however, shows heavy distortion. A spectral analysis of the waveforms used for calculating the noise power (11) revealed that the latter system has a distorted frequency response in the 1.4kHz to 4.00kHz band – affecting more than half of the signal bandwidth. The other systems, however, show no such distortion and posses a flat frequency response as expected.

It is also clear from the signal constellation that there is a random phase rotation that cannot be due to phase noise alone. It is believed that this rotation is due the lack of precision in synchronizing the received time domain signal. At every cycle, the receiver A/D converter samples slightly ahead or behind the exact time required. From the constellation diagram, the overall phase spread in any one quadrant can be calculated and used to infer the related (sampling) time delay. In one such experiment, the delay was calculated to be $16.67\mu s$. This shows that although the delay is within the sampling interval ($125\mu s$), the drift is significant.

IV. Conclusion

The experimental results validate the claim that intensity modulation using OFDM is indeed feasible; the high crest factor that plagues OFDM RF equipment is no longer a disadvantage. The prototype system has managed a distance close to one meter with an impressive bit error rate of 10^{-3} under the moderate ambient light conditions found indoors. This distance has been achieved with a single LED and without any kind of channel or source coding – it is assumed that an array of similar LEDs with error correction coding would have a much higher intensity and achieve much greater distances with an even lower BER. The system performance curves also display a good match between the theoretical results and the experimental data. It is also clear that the system performance is ultimately dependent on the environment; the interference observed from the fluorescent lighting system can be easily mitigated by shifting the system bandwidth to a higher frequency. It is possible to further improve the system performance with a faster DSP, better data coding, a higher number of subcarriers, a larger FFT/IFFT, or any combination of these factors.

References

[1] T. Komine and M. Nakagawa, "Fundamental analysis for visible-light communication system using LED lights," *IEEE Trans. Consumer Electron.*, vol. 50, no. 1, pp. 100–107, Feb. 2004.

[2] Y. Tanaka, T. Komine, S. Haruyama, and M. Nakagawa, "Indoor visible communication utilizing plural white LEDs as lighting," in *The 12th IEEE International Symposium on Personal, Indoor and Mobile Radio Communications (PIMRC 2001)*, San Diego, CA, Sept. 2001, pp. F81–F85.

[3] J. R. Barry, J. M. Kahn, W. J. Krause, E. A. Lee, and D. G. Messerschmitt, "Simulation of multipath impulse response for indoor wireless optical channels," *IEEE J. Select. Areas Commun.*, vol. 11, pp. 367–379, Apr. 1993.

[4] F. R. Gfeller and U. Bapst, "Wireless in-house data communication via diffuse infrared radiation," in *Proceedings of the IEEE*, Nov. 1979, pp. 1474–1486.

[5] T. Komine and M. Nakagawa, "Integrated system of white LED visible-light communication and power-line communication," *The 13th IEEE International Symposium on Personal, Indoor and Mobile Radio Communications (PIMRC 2002)*, vol. 4, pp. 1762–1766, Sept. 2002.

[6] J. R. Barry, *Wireless Infrared Communications*. Boston, MA: Kluwer Academic Press, 1994.